Food Research International xxx (2016) xxx–xxx

Contents lists available at ScienceDirect

Food Research International

journal homepage: www.elsevier.com/locate/foodres

New insights about flocculation process in sodium caseinate-stabilized emulsions

Cristián Huck-Iriart [a], Juan Montes-de-Oca-Ávalos [b,c], María Lidia Herrera [b], Roberto Jorge Candal [a,d,*], Cristiano Luis Pinto-de-Oliveira [e], Iris Linares-Torriani [f]

[a] Escuela de Ciencia y Tecnología, CONICET, Universidad Nacional de San Martín (UNSAM), Campus Miguelete, 25 de Mayo y Francia, 1650 San Martín, Provincia de Buenos Aires, Argentina
[b] Instituto de Tecnología en Polímeros y Nanotecnología (ITPN), Universidad de Buenos Aires (UBA), CONICET, Facultad de Ingeniería, Las Heras 2214, C1127AAQ Buenos Aires, Argentina
[c] Departamento de Química Inorgánica, Analítica y Química Física (DQIAQF), Facultad de Ciencias Exactas y Naturales, Universidad de Buenos Aires, Ciudad Universitaria, Pabellón 2, Piso 3, C1428EHA Buenos Aires, Argentina
[d] Instituto de Investigación e Ingeniería Ambiental, CONICET, Universidad Nacional de San Martín (UNSAM), Campus Miguelete, 25 de Mayo y Francia, 1650 San Martín, Provincia de Buenos Aires, Argentina
[e] Instituto de Física, Universidade de Sao Paulo, Sao Paulo, SP, Brazil
[f] Instituto de Física "Gleb Wataghin", Universidade Estadual de Campinas, Campinas, SP, Brazil

ARTICLE INFO

Article history:
Received 5 June 2016
Received in revised form 13 August 2016
Accepted 20 August 2016
Available online xxxx

Keywords:
Sodium caseinate
Disaccharides
Emulsions
Flocculation
SAXS
Turbiscan

ABSTRACT

Flocculation process was studied in emulsions formulated with 10 wt.% sunflower oil, 2, 5 or 7.5 wt.% NaCas, and with or without addition of sucrose (0, 5, 10, 15, 20 or 30 wt.%). Two different processing conditions were used to prepare emulsions: ultraturrax homogenization or further homogenization by ultrasound. Emulsions with droplets with diameters above (coarse) or below (fine) 1 μm were obtained. Emulsions were analyzed for droplet size distribution by static light scattering (SLS), stability by Turbiscan, and structure by confocal laser scanning microscopy (CLSM) and small angle X-ray scattering (SAXS). SAXS data were fitted by a theoretical model that considered a system composed of poly dispersed spheres with repulsive interaction and presence of aggregates. Flocculation behavior was caused by the self-assembly properties of NaCas, but the process was more closely related to interfacial protein content than micelles concentration in the aqueous phase. The results indicated that casein aggregation was strongly affected by disaccharide addition, hydrophobic interaction of the emulsion droplets, and interactions among interfacial protein molecules. The structural changes detected in the protein micelles in different environments allowed understanding the macroscopic physical behavior observed in concentrated NaCas emulsions.

1. Introduction

Caseins are a family of unstructured amphiphilic milk proteins known as α_{S1}, α_{S2}, β and κ, which have the tendency to naturally form complex aggregates with reported average sizes of up to 300 nm (Livney, 2010). Sodium caseinate (NaCas) results from the removal of calcium phosphate and is widely used in pharmaceutical and food industries as an emulsion stabilizer and foam formation agent. NaCas exists in aqueous solution at neutral pH as a soluble mixture of casein monomers and self-assembled protein aggregates of sizes around 10–20 nm in diameter and molecular weight of ~2.5×10^5 Da, also called nanoparticles in literature (Dickinson, 2006).

Among other factors, the extent of aggregation of NaCas is affected by the presence in the aqueous phase of compounds such as disaccharides. The effect of sucrose on emulsion physical behavior was reported to be strongly dependent on the pH. At neutral pH light scattering studies indicated a reduction in aggregation but at pH close to the isoelectric point (Ip = 4.5) an increase on the radius of gyration was reported (Belyakova et al., 2003; Dickinson, 2006; Ruis, van Gruijthuijsen, Venema, & van der Linden, 2007). These results indicated that sucrose has an important effect on this system and therefore it is also of great interest to investigate how disaccharides modify the structure of sodium caseinate stabilized emulsions.

In order to obtain unbiased results when studying emulsion stability as well as structural properties, the experimental techniques applied have to be as little invasive as possible. Scattering methods are a good example of such techniques and can provide important information on the structural and dynamical properties of heterogeneous fluids

* Corresponding author at: Escuela de Ciencia y Tecnología, CONICET, Universidad Nacional de San Martín (UNSAM), Campus Miguelete, 25 de Mayo y Francia, 1650 San Martín, Provincia de Buenos Aires, Argentina.
E-mail addresses: chinorgchem@gmail.com (C. Huck-Iriart), jmontesdeocaav@gmail.com (J. Montes-de-Oca-Ávalos), mlidiaherrera@gmail.com (M.L. Herrera), rjcandal@gmail.com (R.J. Candal), crislpo@if.usp.br (C.L. Pinto-de-Oliveira), torriani@ifi.unicamp.br (I. Linares-Torriani).

http://dx.doi.org/10.1016/j.foodres.2016.08.026
0963-9969/

(Alexander & Dalgleish, 2006). However, some of those techniques require a substantial dilution of the samples. This dilution disrupts emulsion structures modifying the actual system. Therefore, the ability to study the stability of food emulsions in their undiluted forms may reveal subtle correlations affecting emulsions physical changes. A relatively recently developed technique, the Turbiscan method, allows registration of the turbidity profile of an emulsion along the height of a glass tube filled with the emulsion. The analysis of the turbidity profiles with time leads to quantitative data on the stability of the studied emulsions and allows making objective comparisons between different emulsions (Mengual, Meunier, Cayre, Puech, & Snabre, 1999a). Food emulsions that can be described by the Turbiscan method have droplet sizes typically between 0.1 and 100 μm (Huck-Iriart, Álvarez-Cerimedo, Candal, & Herrera, 2011; Huck-Iriart, Pinzones Ruiz-Henestrosa, Candal, & Herrera, 2013). Small Angle X-Ray Scattering (SAXS) is a non-invasive technique generally used in materials and life science. Due to the short wavelength of X-Rays, this technique provides structural information on colloidal particles and complex fluids in the 1–100 nm size range. Combining both techniques, Turbiscan and SAXS, experimental data may be obtained in a wide range of sizes.

For the correct analysis and interpretation of the SAXS data, a possible approach is to assume a certain model for the system, based on previous knowledge, and compare it with the measured data using least square methods (Pedersen, 1997). In the past, simple models were used to describe milk casein in dilute solution (Holt, Kruif, Tuinier, & Timmis, 2003) and some important structural information was reported. However, in emulsions system, the detailed nature of the molecular interactions involved in the casein micelles formation and the arrangement of the proteins in the casein micellar aggregates is still not completely established. Notwithstanding, the existing data serves as a basis to propose a working micellar model that describes the structure of more complex systems, such as NaCas oil-in-water (O/W) emulsions.

Emulsions are thermodynamically unstable liquid-liquid dispersions. The common strategies to kinetically stabilize these systems involve modification of the liquid-liquid surface tension, the droplet size and the viscosity of the continuum phase (Ivanov & Kralchevsky, 1997). These strategies are not independent since a complex interaction between proteins, surfactants, additives and liquid phases might occur (Jourdain, Schmitt, Leser, Murray, & Dickinson, 2009; Woodward, Gunning, Mackie, Wilde, & Morris, 2009). Stability of sodium caseinate emulsions has been widely investigated (Dickinson, Golding, & Povey, 1997; Hemar et al., 2003; Belyakova et al., 2003; McClements, 2004), to name a few. Flocculation and creaming were the most frequent macroscopic manifestations reported. According to the literature, flocculation occurred above some critical concentration of stabilizing polymer and was sensitive to its concentration. Flocculation was especially related to the excess of unadsorbed protein (Dickinson et al., 1997; Dickinson & Golding, 1997). Although flocculation mechanism was widely investigated, recent studies using non disturbing techniques showed that flocculation process was more complex than reported in literature (Álvarez-Cerimedo, Huck-Iriart, & Herrera, 2010; Huck-Iriart et al., 2013). The results reported in those studies suggest that in sodium caseinate-stabilized emulsions, flocculation is a process that remains fairly poorly understood.

The aim of the present work was to further study flocculation process at the micro and nanoscales from a few nanometers up to hundreds of microns.

2. Materials and methods

2.1. Materials

α,α-Trehalose dihydrate and sucrose from Sigma (Sigma–Aldrich, St. Louis, Mo., USA) were used without any further purification. HPLC water was used for all experimental work. Sodium caseinate (NaCas) was obtained from ICN (ICN Biomedical, Inc., Aurora, Ohio, USA) and used without any further purification. The oil phase was commercial sunflower seed oil (SFO) which main fatty acids were identified as C16:0, C18:0, C18:1, and C18:2 with percentages of 6.7%, 3.6%, 21.9%, and 66.3%, respectively.

2.2. Emulsion preparation

Aqueous phase may contain no sucrose or 5, 10, 15, 20, or 30 wt.% sucrose added to the continuous phase. Oil phase was commercial SFO and in all emulsions represented 10 wt.%. NaCas was used as emulsifier at 2.0, 5.0, and 7.5 wt.% in the aqueous phase. Oil and aqueous phases were mixed using an Ultra-Turrax (UT) T8 high speed blender (S 8 N-5G dispersing tool, IKA Labortechnik, Janke & Kunkel, GmbH & Co., Staufen, Germany), operated at 20,000 rpm for 1 min. Coarse emulsions (UT) were obtained after repeating this process three times. The resultant coarse emulsions were further homogenized for 20 min using an ultrasonic liquid processing (US), VIBRA CELL, VCX model (Sonics & Materials, Inc., Newtown, CT, USA). The temperature of the sample-cell was controlled by means of a water bath set at 15 °C with a temperature cut down control of 40 ± 1 °C during ultrasound treatment. After ultrasound treatment fine emulsions were obtained (UT + US). Then, the samples were cooled quiescently to ambient temperature (22.5 °C). Subsequently they were analyzed for particle size distribution, stability in quiescent conditions and microstructure. The pHs of the SFO emulsions were 6.66 ± 0.05, close to 7. No buffer was added to the emulsions. Experiments were done in duplicate and results were averaged.

2.3. Particle size analysis

The particle size distribution of the emulsions was determined immediately after emulsion preparation by static light scattering (SLS) using a Mastersizer 2000 with a Hydro 2000MU as dispersion unit (Malvern Instruments Ltd., UK). The pump speed was settled at 1800 RPM. Refraction index for the oil phase was 1.4694. Determinations were conducted in duplicate and values of standard deviations were <0.2 μm. Distributions were expressed as differential volume. One of the parameters selected to characterize distributions was the volume-weighted mean diameter ($D_{4,3}$) since it has been reported that it is more sensitive to fat droplet aggregation than Sauter mean diameter ($D_{3,2}$) (Relkin & Sourdet, 2005). Other parameters selected to describe the distribution were distribution width (W) and volume percentage of particles exceeding 1 μm in diameter ($\%V_{d>1}$) (Thanasukarn, Pongsawatmanit, & McClements, 2006).

2.4. Emulsion stability

The stability of the emulsions was analyzed using a vertical scan analyzer Turbiscan MA 2000 (Formulaction, Toulouse, France). This equipment allows the optical characterization of any type of dispersion (Mengual, Meunier, Cayre, Puech, & Snabre, 1999b). A scheme of the equipment was reported in Pan, Tomás, and Añón (2002). The samples were put in a flat-bottomed cylindrical glass measurement cell and scanned from the bottom to the top. The backscattering (BS) and transmission (T) profiles as a function of the sample height (total height = 60 mm) were studied in quiescent conditions at 22.5 °C. The mechanism making the dispersion unstable was deduced from the transmission or the backscattering data. Measurements of the emulsions were performed immediately after preparation and at different time intervals: 2 min per step over the period of 30 min for course emulsions (Ultra Turrax, UT), and twice a day during a week for fine emulsions (UT + Ultrasound, US).

Creaming was detected using the Turbiscan as it induced a variation of the concentration between the top and the bottom of the cell. The curves obtained by plotting ΔBS vs. tube length (where ΔBS is calculated by subtracting the BS profile at t = 0 from the profile at t = t_i, $\Delta BS = BS_{ti} - BS_0$, in the so called reference mode), displayed a typical shape

Please cite this article as: Huck-Iriart, C., et al., New insights about flocculation process in sodium caseinate-stabilized emulsions, *Food Research International* (2016), http://dx.doi.org/10.1016/j.foodres.2016.08.026

with a wide peak at the initial part of the tube (lower zone) between 0 and 20 mm from which the kinetics of migration of small particles was calculated (Mengual et al., 1999b). Peak thickness (peak width) was measured at a fixed value of ΔBS (50% of the maximum height for the most prominent peak). When creaming was the main destabilization mechanism, peak thickness vs. time was fitted with a straight line.

Flocculation was followed by measuring the BS average (BS_{av}) values as a function of storage time in the middle zone of the tube (20–50 mm). This region was the best to evaluate flocculation because it was not affected by creaming of small particles.

2.5. Microstructure

The Olympus FV300 (Olympus Ltd., London, UK) confocal laser scanning microscope (CLSM) with a Ar gas laser (k = 488 nm) was used to collect the images. A 10× ocular was used, together with a 60× objective for a visual magnification of 600×. The laser intensity used was below 20% to avoid photochemical decomposition of the Nile-Red colorant (Sigma Aldrich St. Louis, Mo., USA). Images were recorded by using confocal assistant Olympus Fluoview version 3.3 software provided with the FV300 CLSM. US samples were analyzed immediately after preparation. US + UT samples were kept at 22.5 °C for 24 h before observation.

2.6. Small angle X-ray scattering studies

The SAXS measurements were performed at the DO2A-SAXS2 beamline of the Synchrotron National Laboratory (LNLS, Campinas, Brazil) with a 1.488 Å wavelength. The scattering intensity distributions as a function of scattering vector q were obtained in the q range between 0.0076 and 0.15 $Å^{-1}$. The SAXS patterns were recorded with exposure times of 30 s. A MARCCD 2D detector was used with 2014.73 mm sample detector distance. One-dimensional curves were obtained by integration of the 2D data using the program FIT-2D (Hammersley, Svernsson, Hanfland, Fitch, & Häusermann, 1996). All emulsion systems were kept at room temperature, and then placed in the beamline vacuum-tight temperature-controlled X-ray cell for liquids (Cavalcanti et al., 2004). The SAXS normalized patterns were fitted using an in-house written program.

Data analysis using a simple model composed of homogeneous spherical particles for the primary casein micelles was tested but it did not provide a good fit for the experimental data. The choice of a model that adequately fitted the experimental curves was based on the previously reported neutron scattering experiments describing the primary casein micelles as closely packed protein aggregates with a denser central core and average radius of 7–8 nm (Hansen et al., 1996). The main difference between both models is that neutron model considers polydisperse spheres, which is particularly appropriate for casein micelle systems.

The normalized scattered intensity is generally represented as a function of the reciprocal space momentum transfer modulus q, with $q = (4\pi/\lambda)\sin(\theta)$ where λ is the radiation wavelength and 2θ is the scattering angle. In order to describe the X-ray scattering from the NaCas O/W emulsions, a model composed of polydisperse core shell spheres, as mentioned above, was used to fit the experimental data. In this formulation, the normalized amplitude of the form factor of a core shell spherical particle (Pedersen, 2002) is given by:

$$A_{cs}(q,R) = \frac{V(R+T)\frac{\Delta\rho_{out}}{\Delta\rho_{in}}A_{sph}(q,R+T) - \left(\frac{\Delta\rho_{out}}{\Delta\rho_{in}} - 1\right)V(R)A_{sph}(q,R)}{V(R+T) - \left(\frac{\Delta\rho_{out}}{\Delta\rho_{in}} - 1\right)V(R)} \quad (1)$$

where $\Delta\rho_{out}/\Delta\rho_{in}$ is the ratio between the outer and inner scattering length contrast for the core shell model, T is the shell thickness, $V = 4/3\pi R^3$ is the sphere volume and A_{sph} is the normalized amplitude form factor for a solid sphere given by,

$$A_{sph}(q,R) = \frac{3[\sin(qR) - qR\cos(qR)]}{(qR)^3} \quad (2)$$

The core shell particle model used in our calculations assumes the existence of polydispersity which is taken into account by the distribution function D(R) included in the final expression for the form factor of the polydisperse system (Eq. (3)).

$$P_{CS}(q) = \int D(R)V(R)^2 A_{CS}(q,R)^2 dR \quad (3)$$

For the number size distribution D(R) a Schulz-Zimm normalized distribution (Zimm, 1948) was used which allows the inclusion of a polydispersity function with a variance σ around a size average <R>.

$$D(R) = (A)^B \frac{R^{B-1}}{\Gamma(B)} \exp(-AR)$$
$$A = \frac{<R>}{\sigma^2}$$
$$B = A<R> \quad (4)$$

Correlation between the particles has to be expressed in terms of a structure factor S(q). In the present model the total structure factor was split into two contributions, $S(q) = S_{HS}(q) \cdot S_{agg}(q)$. The first multiplying factor takes into account positional correlations between primary casein micelles. This was accounted for by the use of the Percus-Yevick approximation (Percus & Yevick, 1958) for closure relation which leads to the expression:

$$S_{HS}(q) = \frac{1}{1 + 24\eta G(2R_{HS}q)/(2R_{HS}q)} \quad (5)$$

where,

$$G(w) = \frac{\alpha(\sin w - w\cos w)}{w^2} + \frac{\beta(2w\sin w + (2-w^2)\cos w - 2)}{w^3} + \frac{\gamma[-w^4\cos w + 4\{(3w^2-6)\cos w + (w^3-6w)\sin w + 6\}]}{w^5}$$

and,

$\alpha = \frac{(1+2\eta)^2}{(1-\eta)^4}$, $\beta = \frac{-6\eta(1+\eta/2)^2}{(1-\eta)^4}$, $\gamma = \frac{\eta\alpha}{2}$.

Here, R_{HS} can be understood as an effective hard sphere radius for the core shell particles. In the expression for the total structure factor $S(q) = S_{HS}(q).S_{agg}(q)$, the second multiplying factor S_{agg} accounts for the aggregation of the core-shell spheres. The structure factor for a fractal arrangement of spherical particles was used to account for this interaction (Teixeira, 1988).

$$S_{agg}(q,R) = 1 + \frac{D\Gamma(D-1)}{(qR)^D\left[1 + 1/(q\xi)^2\right]^{(D-1)/2}} \sin\left[(D-1)\tan^{-1}(q\xi)\right] \quad (6)$$

Here, D is the fractal dimension and ξ is the cutoff length for the fractal correlation. In this model, the cutoff length is related to the average size of the larger (supra-micellar) clusters which are formed as a result of the aggregation of the primary casein micelles. The X-ray scattering experiments performed in this study covered a size range of 4–40 nm. Although our SAXS data did not provide information about large clusters resulting from further aggregation of primary casein micelles or other large aggregates that might be formed by any interaction of the casein micelles with the lipid phase droplets in the emulsion, the cutoff length can be understood as a rough estimation of the supra-micellar cluster size. Also, the fractal dimension is indicative of how the protein primary micelles structurally assemble when forming larger aggregates.

Please cite this article as: Huck-Iriart, C., et al., New insights about flocculation process in sodium caseinate-stabilized emulsions, *Food Research International* (2016), http://dx.doi.org/10.1016/j.foodres.2016.08.026

This is important in stability studies of emulsions prepared with proteins and polysaccharides mixtures. Both parameters D and ξ were obtained from the fitting procedure. The final expression that was used to compare the calculated intensity with the experimental data is given by:

$$I(q) = S_C\, P_{CS}(q) S_{HS}(q) S_{agg}(q) + \text{Back} \quad (7)$$

where S_C is an overall scale factor and Back is a constant background. Typical values for all parameters were initially obtained from the fitting procedure. The shell thickness and the effective hard sphere radius (R_{HS}) were fixed for further optimizations. A value of 3 Å was selected for shell thickness because it is close to the value of the hydration shell of the casein monomers and R_{HS} was set as 3x <R>. With these settings, for all samples, <R> values of primary casein micelle in aqueous solutions were close to the ones reported in literature from light scattering techniques indicating that the model predictions were correct. A least squares routine was implemented to fit the experimental data. The list of fitting parameters is shown in Table 1.

2.7. Statistical analysis

For SLS and Turbiscan data, significant differences between means were determined by the Student's *t*-test. An α level of 0.05 was used for significance. Results are reported as mean and standard deviation.

For the SAXS model, parameter "R value" was selected to provide an indicator of the fit quality (Breßler, Kohlbrecher, & Thünemann, 2015). It was calculated using the following equation:

$$\text{R value} = \frac{\sum_{i=1}^{N} \left| |I_{exp}(q_i)| - |I_{mod}(q_i)| \right|}{\sum_{i=1}^{N} |I_{exp}(q_i)|} \quad (8)$$

A R value ranging between 0 and about 0.1 indicates a good to acceptable fit, whereas large values (up to infinity) denote a poor fit.

3. Results and discussion

3.1. Droplet size distribution in O/W emulsions stabilized with NaCas

An emulsion prepared with 10 wt.% sunflower oil and 5 wt.% NaCas was selected as an example for describing the effect of processing treatments and disaccharides addition to the aqueous phase on particle size distribution. Selected particle size distributions are reported in Fig. 1, and $D_{4,3}$, *W*, and $V_{d>1}$ parameters calculated from curves in Fig. 1 are shown in Table 2. The diameters of the droplets present in the UT homogenized emulsions formulated with or without sucrose were in the 10–20 μm range. After US homogenization the diameters of the droplets fell below 1 μm for both formulations. Table 2 clearly showed that US

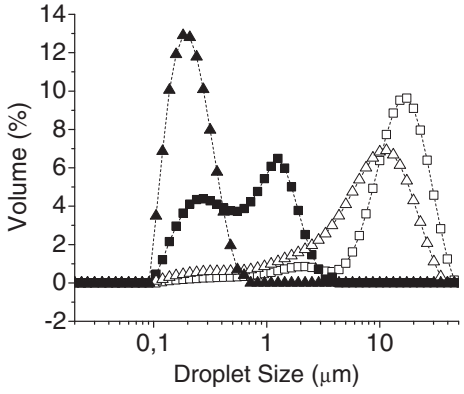

Fig. 1. Particle size distributions of emulsions with 10 wt.% sunflower oil (SFO) as lipid phase and 5 wt.% sodium caseinate (NaCas). Empty symbols: emulsions homogenized by ultraturrax (UT); Solid symbols: emulsions homogenized by ultraturrax and ultrasound (UT + US); Square symbols: emulsions without sucrose added; Triangles: emulsions with 20 wt.% sucrose.

treatment significantly reduce $D_{4,3}$ and $V_{d>1}$ parameters. Distributions for emulsions without sucrose were bimodal. However, when US was applied the population with smaller diameters of the two peaks obtained grew in percentage of total population compared to the UT emulsion. Addition of sucrose to the aqueous phase modified the particle size distribution. The droplet size distributions for the samples without sucrose, that were bimodal, became monomodal after 20 wt.% sucrose addition. Addition of sucrose also produced in both cases (UT or UT + US) narrower profiles than for the same emulsions but without sucrose. This effect was more notorious when US was applied as indicated by parameters $D_{4,3}$, *W*, and $V_{d>1}$ (Table 2). The effect of sucrose may be understood in different ways: It may form hydrogen bonds between hydroxyl groups of sucrose and carboxylic groups of protein or may act as a solvent of protein modifying interactions among protein molecules. According to our previous (Álvarez-Cerimedo et al., 2010; Huck-Iriart et al., 2013) and new results, the major factors affecting the droplet size distribution were: (a) NaCas concentration, (b) the continuous phase composition and (c) the way of processing the sample which may affect the NaCas protein structure and its aggregation topology at the oil-water interface, as discussed in Section 3.4. Particle size is one of the factors strongly related to emulsion stability (Álvarez-Cerimedo et al., 2010). Therefore different destabilization mechanisms may be expected for the selected emulsions.

3.2. Emulsion stability

Fig. 2 reports the changes in BS profiles with time, in reference mode (ΔBS), for samples formulated with 10 wt.% SFO and stabilized by 5 wt.% NaCas. Samples formulated without sucrose were homogenized first by

Table 1
Structural parameters obtained from the SAXS model.

	Description
Unfixed parameter	
SC	Overall scale factor
Back	Constant background
<R>	Average shell inner radius
$\Delta\rho_{out}/\Delta\rho_{in}$	Ratio between the outer and inner scattering length contrast for the core shell model
σ	Width of the polydispersity distribution
D	Fractal dimension
ξ	Fractal cutoff correlation
ϕ_e	Effective volume fraction of the particles
$R_{HS} = 3x$ <R>	Effective hard sphere radius
Fixed parameter	
T = 3 Å	Shell thickness

Table 2
Volume-weighted mean diameter ($D_{4,3}$, μm), width of the distribution (*W*), and volume percentage of particles exceeding 1 μm in diameter ($\%V_{d>1}$) of emulsions formulated with 10 wt.% sunflower oil (SFO), 5 wt.% sodium caseinate (NaCas), and with or without 20 wt.% sucrose (S), homogenized under different processing conditions.

Emulsion	$D_{4,3}$ (μm)	*W* (μm)	$\%V_{d>1}$
UT			
0 wt.% S	16.40 ± 0.21^a	95.61 ± 0.30^a	26.01 ± 0.41^a
20 wt.% S	9.91 ± 0.13^b	91.72 ± 0.41^b	19.26 ± 0.12^b
US			
0 wt.% S	0.76 ± 0.01^c	39.71 ± 0.12^c	1.93 ± 0.01^c
20 wt.% S	0.23 ± 0.01^d	0.01 ± 0.01^d	0.23 ± 0.01^d

Significant differences between means were determined by the Student's *t*-test. An α level of 0.05 was used for significance. Data in the same column with the same superscript are not significantly different.

Please cite this article as: Huck-Iriart, C., et al., New insights about flocculation process in sodium caseinate-stabilized emulsions, *Food Research International* (2016), http://dx.doi.org/10.1016/j.foodres.2016.08.026

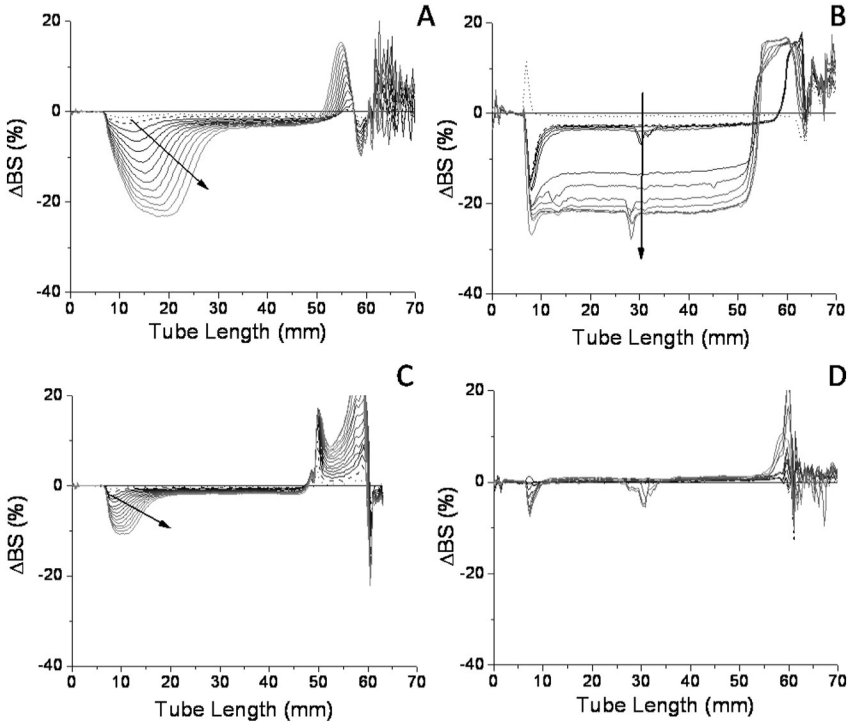

Fig. 2. Back scattering profiles in reference mode ($\Delta BS = BS_{ti} - BS_0$), as a function of tube length for different storage times in quiescent conditions. The arrow denotes time. All emulsions were formulated with 10 wt.% SFO and 5 wt.% NaCas. Without sucrose: A homogenized by UT, B homogenized by UT + US; With 20 wt.% sucrose: C homogenized by UT, D homogenized by UT + US. Abbreviations as in Fig. 1.

UT (A) and further by US (B). Fig. 2C and D shows the effect of addition of 20 wt.% sucrose to the aqueous phase. Part C corresponds to the coarse (UT) and part D to the fine (UT + US) emulsion. For the emulsion in Fig. 2A, the main mechanism of destabilization was creaming of individual particles. This is noticed from the decrease in ΔBS_{ti} at the bottom of the tube (0–20 mm) and a concomitant increase in ΔBS_{ti} in the upper zone (50–65 mm) attributed to the formation of a cream layer. The slope of the linear zone of peak thickness vs. time curve (an estimation of migration rate) was calculated as explained in Section 2.4. Values of slope and correlation coefficient are reported in Table 3. As shown in Fig. 3, selected zone of peak thickness vs. time values may be fitted to a straight line, corroborating that creaming of small particles is the main mechanism of destabilization for emulsion in Fig. 2A. Application of ultrasound treatment modified the main destabilization mechanism changing from creaming to flocculation as noticed by the way in which ΔBS profiles changed with time (Fig. 2B). ΔBS diminished in the range 20–50 mm tube length indicating increase in emulsion particle size with time, which meant that Turbiscan detected particle aggregation. In sucrose containing emulsions, droplet size was significantly smaller than in the case of emulsions formulated without sucrose (Table 2). In addition to producing smaller particle size, sucrose addition to the UT emulsion led to less destabilization and to a lower migration rate than in emulsions without sucrose (Fig. 2C, Table 3). Value of slope of the linear zone of peak thickness with time curve for sugar addition was significantly lower than value for formulation without sucrose (Fig. 3, Table 3). In the case of US treated samples, addition of sucrose allowed obtaining a stable emulsion (Fig. 2D). Fig. 2D clearly shows that sucrose suppressed flocculation.

It was reported that the stability behavior of sodium caseinate-stabilized emulsions was closely related to oil-to-protein ratio (Dickinson & Golding, 1997). According to these authors, the reversible flocculation of emulsion samples of high protein content is readily explicable in terms of depletion flocculation of droplets by unadsorbed protein existing in the form of approximately spherical caseinate submicelles. Our data, however, showed that two emulsions formulated in the same way (Fig. 2A and B), that is, with the same total protein content

Table 3
Slope of the linear zone (mm/h) and correlation coefficients (R^2) evaluated from the kinetics of migration measured from the BS profiles in reference mode in the bottom zone of the tube (0–20 mm) as the peak-thickness with time for emulsions in Fig. 3.

Emulsion	Slope	R^2
UT		
0 wt.% S	58.0 ± 3.0^a	0.988
20 wt.% S	21.0 ± 1.0^b	0.991
US		
0 wt.% S	Flocculation	–
20 wt.% S	Stable emulsion	–

Significant differences between means were determined by the Student's *t*-test. An α level of 0.05 was used for significance. Data in the same column with the same superscript are not significantly different.
R correlation coefficient.

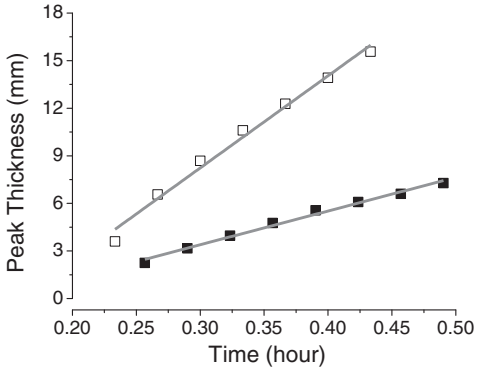

Fig. 3. Linear region of peak thickness with time curves measured at the bottom zone of the tube (0–20 mm tube length) for UT emulsion without sucrose (empty symbol) and UT emulsion with 20 wt.% sucrose (solid symbol). Abbreviations as in Fig. 1.

Please cite this article as: Huck-Iriart, C., et al., New insights about flocculation process in sodium caseinate-stabilized emulsions, *Food Research International* (2016), http://dx.doi.org/10.1016/j.foodres.2016.08.026

but prepared using different processing conditions, destabilized by different mechanisms, creaming (Fig. 2A) or flocculation (Fig. 2B), having the same oil-to-protein ratio. In addition, since droplet sizes were smaller for emulsion in Fig. 2B (Table 2), unadsorbed protein should be lower than for emulsion in Fig. 2A. Kalnin, Ouattara, and Ollivon (2004), demonstrated that the ratio aqueous phase/interface of NaCas in emulsions was depending on the surface area of the interface. Therefore, it would be expected that emulsion in Fig. 2A showed a stronger tendency to flocculation. The behavior described by Turbiscan analysis was the opposite than expected taking into account previous reports in literature. This indicated that interfacial protein should also play an important role in flocculation and that this destabilization mechanism is more complex than described.

3.3. Emulsion microstructure

The confocal laser scanning microscopy (CLSM) images of emulsions formulated with 10 wt.% sunflower oil, 5 wt.% sodium caseinate (NaCas), and with different aqueous phase composition, processed in different conditions are presented in Fig. 4A, B, C, and D. The CLSM results can be correlated with the particle size distributions shown in Fig. 1 and the results of the Turbiscan analysis for the same samples, displayed in Section 3.2, Fig. 2A, B, C, and D.

The 10 wt.% SFO emulsion stabilized with 5 wt.% NaCas without sugar in the aqueous phase and processed by Ultraturrax destabilized mainly by creaming as can be seen in Fig. 2A. This emulsion had the largest mean particle size of the 4 samples reported in Fig. 1 as measured by SLS. In agreement with Turbiscan and particle size analysis, the CLSM image of the emulsion in Fig. 4A shows big droplets with a wide dispersion sizes. When the emulsion in Fig. 4A was further homogenized by ultrasound, the droplet size diminished significantly but the size distribution changed from almost monomodal to bimodal (Fig. 1). This emulsion destabilized mainly by flocculation (Fig. 2B) and, as expected, its CLSM image in Fig. 4B displayed a microstructure formed by flocs.

Sucrose addition diminished droplet sizes (Fig. 1) and slowed down creaming kinetics (Fig. 2D). This result was consistent for all techniques. The CLSM image in Fig. 4C shows an emulsion containing droplets smaller than those observed in Fig. 4A, thus being expected to destabilize with a slower creaming rate. Calculation of the slope of peak thickness with time curve related to migration rate confirmed this hypothesis (Table 3). When the emulsion in Fig. 4C was further homogenized by ultrasound treatment, the average droplet size diminished significantly and a monomodal homogeneous population was obtained (Fig. 1). This emulsion was stable for a week (Fig. 2D). In agreement with these findings the CLSM image in Fig. 4D showed small droplets evenly distributed. The droplet size in sunflower oil emulsions prepared both, by UT or by UT and further homogenized by ultrasound (UT + US), became smaller when sucrose at 20 wt.% was added. Addition of sugars also suppressed flocculation after ultrasonic treatment. These results show the relevance of microstructure in emulsion stability which is also closely related to the casein micelles structure, as will be discussed in the next section.

3.4. SAXS measurements

Since the oil droplets in the samples under study are very large, their scattering contribution cannot be detected in the q-range measured in our experiments. Therefore the SAXS signal is mainly caused by the protein micelles in solution. The complex model used in the fitting calculations was based on the existence of three major contributions on the

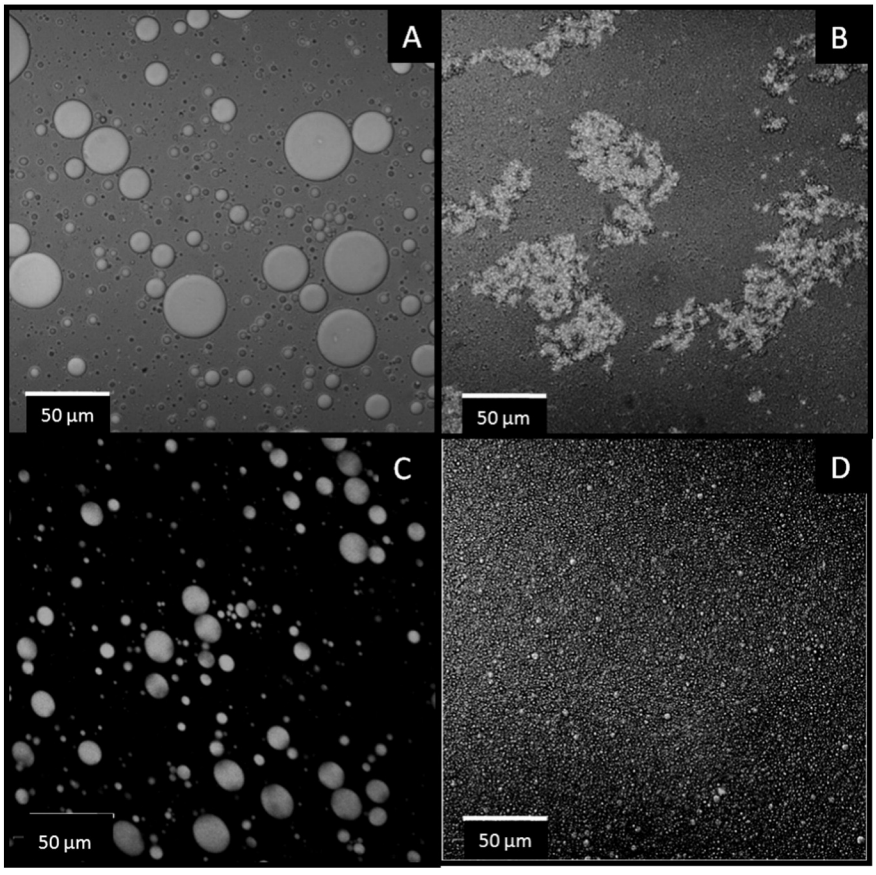

Fig. 4. Confocal laser scattering microscopy (CLSM) images of emulsions with 10 wt.% SFO and 5 wt.% NaCas. Without sucrose: A homogenized by UT, B homogenized by UT + US; With 20 wt.% sucrose: C homogenized by UT, D homogenized by UT + US. Abbreviations as in Fig. 1.

Please cite this article as: Huck-Iriart, C., et al., New insights about flocculation process in sodium caseinate-stabilized emulsions, *Food Research International* (2016), http://dx.doi.org/10.1016/j.foodres.2016.08.026

SAXS data. Fig. 5A shows the contribution of each factor considered in the calculated intensity, I(q) (Eq. (7)). The analyzed sample was the emulsion formulated with 5 wt.% NaCas. At higher angles, the spherical core shell form factor from the primary casein micelles was predominant while at very low angles the contribution from the micellar aggregates was more noticeable, causing an upturn in the scattering curves. The intermediate zone presented a visible broad peak that can be attributed to the primary caseine micelles correlation (S_{HS}). Any correlation existing among the supra-micellar aggregates could only be appreciable at very small angles, in regions inaccessible to our experiment. Therefore, this scattering contribution was not included in the model. However, the presence of the abovementioned regions in the experimental curve allowed proposing a working model from which parameters describing aggregation were extrapolated. The goodness of the full curve fitting indicated that reliable parameters can be calculated.

Fig. 5B reports the normalized intensity vs. scattering vector q for UT emulsions formulated with 10 wt.% SFO, 2.0, 5.0 or 7.5 wt.% NaCas, without sucrose added to the aqueous phase. Experimental data are indicated with symbols and calculated values with a continuous line. The maximum of the hard sphere structure factor (S_{HS}) shifted to higher q values as the sodium caseinate concentration increases. This result was previously described in the literature (Kalnin, Quennesson, Artzner, Schafer, Narayanan & Ollivon, 2004; Kalnin, Ouattara & Ollivon, 2004). The shift to higher q values suggested that primary casein micelles should be smaller or that distances among primary casein micelles should be shorter as the concentration of sodium caseinate increased. Fig. 5C and D report the normalized intensity vs. scattering vector q for emulsions formulated with 10 wt.% SFO and 5.0 wt.% NaCas with and without sucrose homogenized by UT and UT + US, respectively. It can be observed from experimental data that the maximum intensity of the broad peak decreased with sucrose concentration and with ultrasound treatment. More insight about primary micelle correlation can be obtained after the analysis of the contribution of the calculated structure factors. Fig. 6 shows the total structure factor (A) as well as its two separate contributions $S_{HS}(q)$ (B) and $S_{agg}(q)$ (C) for the SFO emulsions formulated with 5 wt.% NaCas reported in Fig. 1. Addition of sugar or application of US to the UT emulsion shifted the position of the maximum $S_{HS}(q)$ to lower values of q. Primary casein micelles correlation was almost lost when 20 wt.% sucrose was added to the emulsion prepared by UT + US treatments. It should be noted that at the highest concentration of sucrose (30 wt.%), micelle correlation was completely lost (Fig. 5D). On the other hand, comparison of the samples with the same sodium caseinate concentration showed that $S_{agg}(q)$ shifted to higher values upon sugar addition or when homogenized by UT + US treatments suggesting the loss of supra micellar correlation. These changes in correlation between the primary casein micelles and among supra micellar aggregates were closely related to sugar concentration, and may be the consequence of the interaction of sucrose with casein. The presence of sucrose decreased the protein-protein interaction, hindering the aggregation of the casein. The application of US helped the dispersion of the aggregates and supra-structures formed by the aggregation of primary casein micelles. It is worth to mention that the loss of correlation corresponded to a marked diminution in size of droplets of the emulsions as can be deduced by comparison of Fig. 5. C and D with Fig. 1 and Fig. 4. These issues will be discussed further.

Experimental data reported in Fig. 5 were evaluated with the proposed model. Table 4 summarizes numerical values of the main parameters obtained from the curve fitting using the model described in Section 2.6. The internal radii <R> obtained from the core shell model calculations were around 4.0 ± 0.2 nm for all samples. The average Schulz-Zimm variance, for all experiments, was 2.0 ± 0.3 nm, which corresponded to a large polydispersity of 50%. A plot of the particle volume distribution shows that up to 60% of the particles are between 5 and 10 nm with an average radius of 7.0 nm (data not shown). In all cases the fractal dimension D is around 3, indicating that the arrangement of the nanoclusters evolves to form a volume fractal (or an interfacial 3D network). Interestingly, the results indicated that the core shell form factor had no significant changes with formulation or homogenization treatment as regards its defining parameters (R, T and σ)

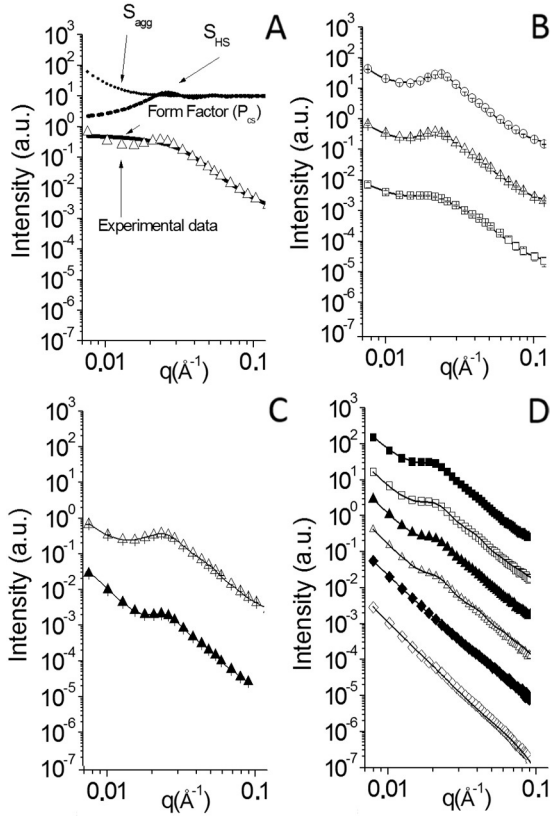

Fig. 5. (A) Separate graphs of the calculated form factor (P_{cs}), (solid line), hard sphere structure factor (S_{HS}), (dashed line), structure factor contribution due to large aggregates (S_{agg}), (dotted line) for the 5 wt.% NaCas stabilized emulsion homogenized by UT. Experimental data are indicated with empty symbols. (B) Normalized intensity vs. scattering vector q for emulsions homogenized by UT, formulated with 10 wt.% SFO. Without sucrose added to the aqueous phase, and stabilized by 2.0 (□), 5.0 (△), or 7.5 (○) wt.% NaCas. Experimental data: empty symbols; proposed model fitting: continuous line. The curves where shifted for clarity. (C) Normalized intensity vs. q for the 5 wt.% NaCas emulsion homogenized by UT. Empty symbol: no sucrose added. Solid symbol: 20 wt.% sucrose. Experimental data: symbols; proposed model fitting: continuous line. (D) Normalized intensity vs. q for emulsions homogenized by UT + US, formulated with 10 wt.% SFO, 5 wt.% NaCas, and different levels of sucrose in the aqueous phase: ■ 0 wt.%, □ 5 wt.%, ▲ 10 wt.%, △ 15 wt.%, ♦ 20 wt.%, and ◇ 30 wt.% sucrose. Experimental data: symbols; proposed model fitting: continuous line. Abbreviations as in Fig. 1.

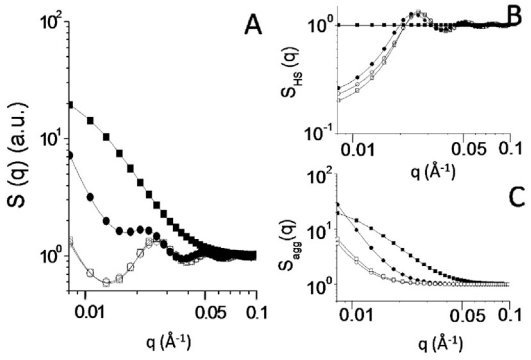

Fig. 6. Structure factors calculated for emulsions formulated with 10 wt.% SFO and 5 wt.% NaCas. Empty symbols: homogenized by UT; full symbols: homogenized by UT + US. Circles: 0 wt.% sucrose; squares: 20 wt.% sucrose. (A) Total structure factors: $S(q) = S_{HS}(q) \cdot S_{agg}(q)$. (B) $S_{HS}(q)$: hard sphere structure factors for casein micelles. (C) $S_{agg}(q)$: structure factors due to large aggregates.

Please cite this article as: Huck-Iriart, C., et al., New insights about flocculation process in sodium caseinate-stabilized emulsions, *Food Research International* (2016), http://dx.doi.org/10.1016/j.foodres.2016.08.026

Table 4
Parameters that best fit the experimental data of I vs. q using Eq. (7). The shell thickness (T) was fixed at 3 Å and the effective hard sphere radius considered for the optimization was $R_{HS} = 3x <R>$.

Sample	<R> (nm)	$\Delta\rho_{out}/\Delta\rho_{in}$	Φ_e	σ (nm)	D	ξ (nm)	R value[a]
Solutions							
5 wt.% NaCas							
0 wt.% S	4.18 ± 0.02	−1.2 ± 0.01	0.21 ± 0.01	2.35 ± 0.04	3.02 ± 0.01	560 ± 70	0.023
20 wt.% S	3.92 ± 0.03	−1.2 ± 0.03	0.24 ± 0.01	2.13 ± 0.05	3.02 ± 0.01	200 ± 20	0.025
Emulsions							
UT							
2 wt.% NaCas							
0 wt.% S	3.91 ± 0.04	−1.0 ± 0.1	0.19 ± 0.01	1.8 ± 0.2	2.96 ± 0.01	600 ± 200	0.042
20 wt.% S	4.10 ± 0.05	−1.7 ± 0.2	0.16 ± 0.01	1.8 ± 0.02	3.07 ± 0.08	400 ± 100	0.012
5 wt.% NaCas							
0 wt.% S	3.90 ± 0.04	−1.2 ± 0.01	0.22 ± 0.01	2.03 ± 0.02	3.00 ± 0.02	480 ± 40	0.017
20 wt.% S	3.96 ± 0.02	−0.11 ± 0.07	0.24 ± 0.01	2.14 ± 0.02	3.17 ± 0.05	380 ± 30	0.062
7.5 wt.% NaCas							
0 wt.% S	3.78 ± 0.02	−0.9 ± 0.1	0.24 ± 0.01	2.26 ± 0.03	3.03 ± 0.01	260 ± 10	0.058
20 wt.% S	3.89 ± 0.01	−1.0 ± 0.1	0.28 ± 0.01	1.82 ± 0.05	3.1 ± 0.1	200 ± 10	0.058
US							
5 wt.% NaCas							
0 wt.% S	4.0 ± 0.1	−0.8 ± 0.02	0.21 ± 0.01	2.69 ± 0.01	3.03 ± 0.02	74 ± 5	0.052
5 wt.% S	4.2 ± 0.1	−0.8 ± 0.02	0.21 ± 0.01	2.75 ± 0.01	3.00 ± 0.01	72 ± 3	0.012
10 wt.% S	4.1 ± 0.1	−0.8 ± 0.02	0.21 ± 0.01	2.70 ± 0.04	3.00 ± 0.01	39 ± 2	0.012
15 wt.% S	4.1 ± 0.1	−0.8 ± 0.02	0.20 ± 0.01	2.71 ± 0.04	3.00 ± 0.01	23 ± 5	0.016
20 wt.% S	3.8 ± 0.1	−0.8 ± 0.02	0.0 ± 0.0	2.3 ± 0.1	3.00 ± 0.01	7 ± 3	0.015
30 wt.% S	3.9 ± 0.1	−0.8 ± 0.02	0.0 ± 0.0	2.3 ± 0.1	3.00 ± 0.01	7 ± 5	0.027

[a] R value was calculated as explained in Section 2.7.

(Table 4). This indicated that this simple form factor is capable of describing the primary casein micelles in all the emulsions or solutions studied. In other words, there were no significant changes in the NaCas micellar structure in aqueous solution or in any of the emulsions with or without additives. On the other hand, there were important changes on the total structure factor, depending on the sample composition. The core shell hard sphere radius R_{HS} and the fractal cutoff correlation length (ξ) provided information on the average distance between the primary casein micelles and on the order of magnitude of the overall micellar aggregates size, respectively. These parameters allowed describing the NaCas aggregates as a function of the environment. R_{HS} showed negligible variation with the environment but ξ was notably affected by emulsion composition and homogenization treatment. Table 4 summarizes values of ξ for solutions and emulsions homogenized under different processing treatments and with different compositions of the aqueous phase. The greatest ξ corresponded to 5 wt.% NaCas solution without sucrose. Emulsions showed smaller values of ξ than solutions in all cases indicating that hydrophobic interaction between protein and the oil phase led to aggregation loss. There are about two orders of magnitude between the NaCas ξ values in emulsions with sugar when compared with UT emulsions without sugar. The effect of sugar is enhanced when the oil-water interface is increased by ultrasonic treatment (Table 4). For US formulations with 20 or 30 wt.% sucrose, the correlation almost disappeared (Fig. 5D) and the ~7 nm calculated ξ value was the only remaining effect. Consequently, most of the supra-micellar structure is lost. These analyses are consistent with the changes in S_{HS} with composition and homogenization treatment discussed above. Our results indicated that the NaCas aggregation loss is produced by simple sugar addition, most likely because sucrose affected protein-protein interactions as mentioned before. The most evident consequence of the loss of aggregation is the appearance of smaller droplets in the emulsions, as determined by SLS (Fig. 1) and CLSM (Fig. 4). In agreement with these results, experimental measurements in similar systems showed that addition of sucrose strongly diminished oil-water surface tension (Huck-Iriart et al., 2013).The decrease in droplets size led to a stable emulsion (Fig. 2D) due to loss of protein ability to aggregate as a consequence of interactions sucrose/casein.

The change in behavior observed in the scattering curves in the case of emulsions (Fig. 5B, C, and D) is an experimental evidence of the synergistic effects that appear as a result of the combination of disaccharides and proteins at the oil/water interface, causing an important decrease of ξ values. Values of ξ for solutions with sucrose were in agreement with the hydrodynamic radii of the NaCas micellar aggregates in solutions, as measured by light scattering techniques, reported in literature (Belyakova et al., 2003). This correlation provided evidence that this model allowed calculating reliable parameters.

The results obtained by light scattering and SAXS techniques confirmed that there was no direct correlation between flocculation and primary micelle aggregation capability in the aqueous phase. The 5 wt.% NaCas emulsion homogenized by UT + US had a low value of parameter ξ (Table 4). However, for this emulsion the main mechanism of destabilization was flocculation (Fig. 2B). UT emulsion without sucrose had one of the highest ξ values (Table 4); however, this emulsion destabilized mainly by creaming (Fig. 2A). Therefore, flocculation is a process more complex than described in literature and it is related to the capability of aggregation of protein molecules at the interface as well as in the aqueous phase. Flocculation occurred as a result of the combination of several factors. Among them, homogenization process that defined droplets size distribution and aggregation topology of protein at the oil-water interface are very relevant and were not considered in literature.

4. Conclusions

In this work we described structural changes of the NaCas micellar and supra-micellar entities present in emulsions with different formulations and their relation to the emulsion macroscopic properties. New correlations were obtained from the results of light scattering based methods, confocal microscopy and SAXS measurements. This last technique provided structural parameters of the O/W emulsion that were not previously reported and new information about protein aggregation behavior that is very relevant to flocculation mechanism was obtained. More experimental evidence at the molecular level of the effect of disaccharides on sodium caseinate micelles and their aggregation properties was also found. The nanoscopic interpretation provided was necessary for explaining emulsion physical behavior at the microscopic level. SAXS was a very useful tool for this investigation and the analysis of the SAXS data provided a good model for the determination of structural parameters of the casein primary micelles and their supra-micellar

Please cite this article as: Huck-Iriart, C., et al., New insights about flocculation process in sodium caseinate-stabilized emulsions, *Food Research International* (2016), http://dx.doi.org/10.1016/j.foodres.2016.08.026

aggregates in the O/W environment. This study allowed obtaining a deeper insight of flocculation process than previously reported. The important decrease in the fractal cutoff correlation length obtained from SAXS data confirmed the molecular interaction of disaccharides and proteins at the oil/water interface and in the aqueous solution. This interaction explained why flocculation can be controlled by suppression of protein aggregation upon sugar addition. A 20 wt.% sucrose addition to fine emulsions allowed obtaining a stable emulsion. Our results proved that the flocculation regime was preponderant when the emulsion droplet size distribution was below one micron and NaCas concentration was above 2 wt.%. On the other hand, when gravitational forces overcame protein-protein interactions, emulsions destabilized by creaming. Flocculation was a consequence of the capability of aggregation of NaCas molecules determined by total protein content, interactions protein/oil at the interface, protein/sucrose in the aqueous phase, droplets size distribution and aggregation topology of protein at the oil-water interface.

Acknowledgments

María L. Herrera and Roberto J. Candal are researchers of the National Research Council of Argentina (CONICET). This work was supported by CONICET through Project PIP 11220110101025, the National Agency for the Promotion of Science and Technology (ANPCyT) through Project PICT 2013-0897, and by the University of Buenos Aires through Project UBA-20020130100136BA. Iris L. Torriani is a I-B researcher of the Brazilian National Research Council (CNPq). CLPO was supported by FAPESP (Proj. # 2010/09277-7) and CNPq. The authors wish to thank the Synchrotron Light National Laboratory (LNLS, Campinas, Brazil) for the use of the SAXS facilities through project D11A-SAXS1-14296.

References

Alexander, M., & Dalgleish, D. G. (2006). Dynamic light scattering techniques and their applications in food science. *Food Biophysics*, *1*, 2–13.

Álvarez-Cerimedo, M. S., Huck-Iriart, C., Candal, R. J., & Herrera, M. L. (2010). Stability of emulsions formulated with high concentrations of sodium caseinate and trehalose. *Food Research International*, *43*, 1482–1493.

Belyakova, L. E., Antipova, A. S., Semenova, M. G., Dickinson, E., Merino, L. M., & Tsapkina, E. N. (2003). Effect of sucrose on molecular and interaction parameters of sodium caseinate in aqueous solution: Relationship to protein gelation. *Colloids and Surfaces B: Biointerfaces*, *31*, 31–46.

Breßler, I., Kohlbrecher, J., & Thünemann, A. F. (2015). *SASfit*: A tool for small-angle scattering data analysis using a library of analytical expressions. *Journal of Applied Crystallography*, *48*, 1587–1598.

Cavalcanti, L. P., Torriani, I. L., Plivelic, T. S., Oliveira, C. L. P., Kellermann, G., & Neuenschwander, R. (2004). Two new sealed sample cells for small-angle X-ray scattering from macromolecules in solution and complex fluids using synchrotron radiation. *Review of Scientific Instruments*, *75*, 4541–4546.

Dickinson, E. (2006). Structure formation in casein-based gels, foams, and emulsions. *Colloids and Surfaces A: Physicochemical and Engineering Aspects*, *288*, 3–11.

Dickinson, E., & Golding, M. (1997). Depletion flocculation of emulsions containing unadsorbed sodium caseinate. *Food Hydrocolloids*, *11*, 13–18.

Dickinson, E., Golding, M., & Povey, M. J. W. (1997). Creaming and flocculation of oil-in-water emulsions containing sodium caseinate. *Journal of Colloid and Interface Science*, *185*, 515–529.

Hammersley, A. P., Svernsson, O. S., Hanfland, M., Fitch, A. N., & Häusermann, D. (1996). Two-dimensional detector software: From real detector to idealised image or two theta scan. *High Pressure Research*, *14*, 235–248.

Hansen, S., Bauer, R., Lomholt, S. B., Bruun-Qvist, K., Pedersen, J. S., & Mortensen, K. (1996). Structure of casein micelles studied by small-angle neutro scattering. *European Biophysics Journal*, *24*, 143–147.

Hemar, Y., Pinder, D. N., Hunter, R. J., Singh, H., Hébraud, P., & Horne, D. S. (2003). Monitoring of flocculation and creaming of sodium-caseinate-stabilized emulsions using diffusing-wave spectroscopy. *Journal of Colloid and Interface Science*, *264*, 502–508.

Holt, C., Kruif, C. G., Tuinier, R., & Timmis, P. A. (2003). Substructure of bovine casein micelles by small-angle X-ray and neutron scattering. *Colloids and Surfaces A: Physicochemical and Engineering Aspects*, *213*, 275–284.

Huck-Iriart, C., Álvarez-Cerimedo, M. S., Candal, R. J., & Herrera, M. L. (2011). Structures and stability of lipid emulsions formulated with sodium caseinate. *Current Opinion in Colloid & Interface Science*, *16*, 412–420.

Huck-Iriart, C., Pinzones Ruiz-Henestrosa, V. M., Candal, R. J., & Herrera, M. L. (2013). Effect of aqueous phase composition on stability of sodium caseinate/sunflower oil emulsions. *Food and Bioprocess Technology*, *6*, 2406–2418.

Ivanov, I. B., & Kralchevsky, P. A. (1997). Stability of emulsions under equilibrium and dynamic conditions. *Colloids and Surfaces A: Physicochemical and Engineering Aspects*, *128*, 155–175.

Jourdain, L. S., Schmitt, C., Leser, M. E., Murray, B. S., & Dickinson, E. (2009). Stability of emulsions containing sodium caseinate and dextran sulfate: Relationship to complexation in solution. *Langmuir*, *25*, 10026–10037.

Kalnin, D., Ouattara, M., & Ollivon, M. (2004a). A new method for the determination of the concentration of free and associated sodium caseinate in model emulsions. *Progress in Colloid and Polymer Science*, *128*, 207–211.

Kalnin, D., Quennesson, P., Artzner, F., Schafer, O., Narayanan, T., & Ollivon, M. (2004b). Monitoring both fat crystallization and self-assembly of sodium caseinate in model emulsions using synchrotron X-ray diffraction. *Progress in Colloid and Polymer Science*, *126*, 139–145.

Livney, Y. D. (2010). Milk proteins as vehicles for bioactives. *Current Opinion in Colloid & Interface Science*, *15*, 73–83.

McClements, D. J. (2004). Protein-stabilized emulsions. *Current Opinion in Colloid & Interface Science*, *9*, 305–313.

Mengual, O., Meunier, G., Cayre, I., Puech, K., & Snabre, P. (1999a). Characterisation of instability of concentrated dispersions by a new optical analyser: The Turbiscan MA 1000. *Colloids and Surfaces A: Physicochemical and Engineering Aspects*, *152*, 111–123.

Mengual, O., Meunier, G., Cayre, I., Puech, K., & Snabre, P. (1999b). TURBISCAN MA 2000: Multiple light scattering measurements for concentrated emulsion and suspension instability analysis. *Talanta*, *50*, 445–456.

Pan, L. G., Tomás, M. C., & Añón, M. C. (2002). Effect of sunflower lecithins on the stability of water-in-oil and oil-in-water emulsions. *Journal of Surfactants and Detergents*, *5*, 135–143.

Pedersen, J. S. (1997). Analysis of small-angle scattering data from colloids and polymer solutions: Modeling and least-squares fitting. *Advances in Colloid and Interface Science*, *70*, 171–201.

Pedersen, J. S. (2002). Modelling of small-angle scattering data from colloids and polymer systems. In P. Lindner, & T. Zemb (Eds.), *Neutrons, X-rays and light* (pp. 391–420). Amsterdam: Elsevier Science B.V.

Percus, J. K., & Yevick, G. (1958). Analysis of classical statistical mechanics by means of collective coordinates. *Physical Review*, *110*, 1–13.

Relkin, P., & Sourdet, S. (2005). Factors affecting fat droplet aggregation in whipped frozen protein-stabilized emulsions. *Food Hydrocolloids*, *19*, 503–511.

Ruis, H. G. M., van Gruijthuijsen, K., Venema, P., & van der Linden, E. (2007). Transitions in structure in oil-in-water emulsions as studied by diffusing wave spectroscopy. *Langmuir*, *23*, 1007–1013.

Teixeira, J. (1988). Small-angle scattering by fractal systems. *Journal of Applied Crystallography*, *21*, 781–785.

Thanasukarn, P., Pongsawatmanit, R., & McClements, D. J. (2006). Utilization of layer-by-layer interfacial deposition technique to improve freeze-thaw stability of oil-in-water emulsions. *Food Research International*, *39*, 721–729.

Woodward, N. C., Gunning, A. P., Mackie, A. R., Wilde, P. J., & Morris, V. J. (2009). Comparison of the orogenic displacement of sodium caseinate with the caseins from the air–water interface by nonionic surfactants. *Langmuir*, *25*, 6739–6744.

Zimm, B. H. J. (1948). The scattering of light and the radial distribution function of high polymer solutions. *Chemical Physics*, *16*, 1093–1116.

Please cite this article as: Huck-Iriart, C., et al., New insights about flocculation process in sodium caseinate-stabilized emulsions, *Food Research International* (2016), http://dx.doi.org/10.1016/j.foodres.2016.08.026